Bull. Chem. Soc. Ethiop. **2008**, 22(3), 423-432. ISSN 1011-3924
Printed in Ethiopia © 2008 Chemical Society of Ethiopia

HYDRATION OF Cd(II): MOLECULAR DYNAMICS STUDY

Ahmed M. Mohammed*

Department of Chemistry, Addis Ababa University, P. O. Box 1176, Addis Ababa, Ethiopia

(Received December 17, 2007; revised June 22, 2008)

ABSTRACT. An ab initio two-body potential and a function correcting for 3-body effects for Cd(II)-water system are constructed. The hydration structure of Cd(II) has been studied by means of molecular dynamics simulations. The inclusion of the three-body correction was found to be crucial for the description of the system, and results thus obtained are in good agreement with experimental values. Radial distribution functions, coordination number distributions, and various angular distributions have been used to discuss details of the hydration structure, together with bond lengths and bond angles of the water molecules in the first hydration shell. The Cd(II) is found 6-fold coordinated. Water molecules in the first hydration shell are shown to be polarized compared to the gas-phase structures. Umbrella-sampling molecular dynamics simulations were performed to investigate the water exchange reaction of Cd(II) ion in aqueous solution. The water-exchange rate constant at 298 K is estimated by the transition state theory to be 4.9 x 10^8 s^{-1}, assuming a transmission coefficient of unity.

KEY WORDS: Molecular dynamics, Umbrella sampling, Hydration structure, Cd(II), Water exchange, Three-body corrections

INTRODUCTION

Knowledge of the structural and dynamical properties of metal ion-water complexes in aqueous solutions is required in many fields of chemistry, biochemistry, and chemical engineering [1-5] and has been the subject of a large number of investigations [6-22].

Classical computer simulation methods particularly molecular dynamics (MD) have been suitable theoretical tools for understanding and predicting the physicochemical properties of ions in solutions at the microscopic level [6, 7, 9-22]. The hydration structures of metal ions predominantly the first hydration shell has been studied by MD method with varying degrees of success depending on the type of metal under study and on ion-solvent interaction potential. It has also been used to study water exchange dynamics of the first hydration shell, however, it was hampered due to the fact that water exchange processes of many metal ions often occur on timescales larger than the nanosecond range typical for ordinary MD simulations. Therefore, observing the transition state is quite rare during a simulation leading to unreliable results. Nevertheless, a biasing function driving particles along a chosen reaction coordinate may be applied in order to increase the probability of finding high-energy states and hence enhancing sampling efficiency in a specific region of phase space.

One powerful approach to adequately sample high energy, i.e. a transition state, is the umbrella-sampling technique [23, 24], which has been widely used to calculate reaction profiles for chemical processes in solution and recently its application for the study water exchange dynamics around metal ions is reported [19-21]. In this technique, a suitable reaction coordinate is chosen and a series of independent simulations are performed by spanning the relevant phase space of the reaction coordinate. A biasing potential is imposed to restrain the system to the desired point on the reaction coordinate, and the potential parameters are forced to change for a series of simulations along an assumed reaction coordinate. To obtain the unbiased free energy profile several methods are available, however, the most common and successful method is the weighted-histogram-analysis method (WHAM) [25-27] which is adopted in this study. By this procedure the potential of mean force (PMF) along the chosen reaction coordinate may be obtained.

*Corresponding author. E-mail: am_moha@chem.aau.edu.et

Water exchange rate constants of most transition metal ions have been investigated by nuclear magnetic resonance (NMR) [7]. There are, however, several cations such as Cd(II) ion, for which water-exchange rate constants are inaccessible by direct measurement. The d^{10} Cd(II) ion is diamagnetic, and NMR cannot be applied with success to study its very fast water-exchange rates. Therefore, theoretical methods are necessary to supplement data from experimental studies.

In this study, 2-body potential for Cd(II)-H_2O interaction and its 3-body correction terms were evaluated by means of *ab inito* molecular orbital calculations and corresponding analytical functions were constructed. Unbiased MD simulation was carried out for Cd(II) in water using the 2-body potential and the 3-body correction function to study hydration structure of the Cd(II) ion. Umbrella-sampling MD simulations using same potentials have been applied to determine the potential force of mean (PMF) for the water-exchange dynamics of Cd(II) in the first hydration shell.

COMPUTATIONAL DETAILS

Construction of ion-water pair potential

Ab initio molecular orbital calculations were carried out at the restricted Hartree-Fock (RHF) level using the Gaussian98 program [28]. The ECP basis set of Christiansen *et al.* [29] for Cd(II) and the DZP basis sets of Dunning [30] for water were employed. Previous investigations have proven that ECP basis sets for the central ion and the DZP basis set for the solvent constitute a satisfactory compromise between accuracy and efficiency [16, 17]. The basis set superposition error (BSSE) was shown to be very small for comparable ions [22]. The experimental gas-phase geometry of H_2O was fixed with the O–H distance of 0.9601 Å and the H–O–H angle of 104.47° [31].

To calculate 2-body interaction energies between Cd(II) and H_2O, the position of the Cd(II) ion was varied around the H_2O molecule by fixing the O atom at the origin, two H atoms on the *xz* plane, and the C_{2v} axis of H_2O on the *z* axis of the Cartesian coordinate system. The values of the Cd–O distance (r_{CdO}), the angle between the O–Cd vector and the *z* axis (θ), and the angle between the *x* axis and the projection of the O–Cd vector onto the *xy* plane (ϕ) were varied over the ranges 1.5 Å $\leq r_{CdO} \leq$ 12.0 Å, $0° \leq \theta \leq 180°$, and $0° \leq \phi \leq 90°$, respectively. The 2-body interaction energies (E_{2bd}) were calculated by subtracting the SCF energies (E_{Cd} and E_W) of isolated Cd(II) and H_2O from that (E_{CdW}) of $[Cd(H_2O)]^{2+}$, as expressed by equation 1.

$$E_{2bd} = E_{CdW} - (E_{Cd} + E_W) \tag{1}$$

A total of 11700 configurations were generated for SCF-energy calculations of $[Cd(H_2O)]^{2+}$ to cover the whole configuration space. To represent the E_{2bd} values by an analytical function, various functions were tested to fit to the E_{2bd} values by a least-squares optimization using the Levenberg-Marquardt algorithm. The best reproducibility was obtained using a function composed of four r^{-m} terms for the non-Coulombic interaction in addition to the Coulombic interaction, as expressed by equation 2,

$$E_{2bd} = \frac{Q_{Cd}Q_O}{r_{CdO}} + A_O r_{CdO}^{-5} + B_O r_{CdO}^{-8} + C_O r_{CdO}^{-9} + D_O r_{CdO}^{-12} + \sum_{i=1}^{2}\left(\frac{Q_{Cd}Q_{H_i}}{r_{CdH_i}} + A_H r_{CdH_i}^{-5} + B_H r_{CdH_i}^{-8} + C_H r_{CdH_i}^{-9} + D_H r_{CdH_i}^{-12} \right) \tag{2}$$

where Q means the atomic net charge, r_{CdH} is the distance between Cd and H, and A, B, C, and D are optimization parameters. The values of -0.6596 and 0.3298 were adopted for Q_O and Q_H, respectively, from the central-force (CF) model for H_2O [32]. The value of Q_{Cd} was assumed to be 2. E_{2bd} values near the global energy minimum were emphasized during the least-squares procedure by assigning an appropriate weighting factor. E_{2bd} values above 30 kcal mol^{-1} were excluded in the optimization of the function. The optimized potential parameters are given in Table 1. The average absolute residual of the fit was 1.3 kcal mol^{-1}. The global energy minimum of the fitted function was found to be -70.4 kcal mol^{-1} at r_{CdO} = 2.14 Å and $\theta = \phi = 0°$.

Construction of 3-body correction term

The 3-body correction energy (E_{3bd}) was calculated according to equation 3,

$$E_{3bd} = E_{CdW_iW_j} - (E_{Cd} + 2E_W) - (E_{CdW_i} + E_{CdW_j}) - E_{W_iW_j} \quad (3)$$

where $E_{CdW_iW_j}$ is the SCF energy for $[Cd(H_2O)_2]^{2+}$, E_{CdW_i} and E_{CdW_j} are the 2-body interaction energies, calculated using the previously developed analytical function (equation 2), and $E_{W_iW_j}$ is the intermolecular potential between H_2O molecules computed using the CF2 model [33]. The SCF-energy calculations were performed by varying independently both Cd–O distance ($2.0 \le r_{CdO} \le 6.0$ Å) and the O–Cd–O angle ($60° \le \psi \le 180°$). The dipole moments of both H_2O molecules were fixed to point toward the Cd(II) ion for all configurations.

Almost all of the E_{3bd} values were found to be positive for the geometries employed in this study. The E_{3bd} value decreases with increasing r_{CdO} and becomes almost 0 kcal mol^{-1} when either r_{CdO} approaches to 6.0 Å. Furthermore, given a set of two r_{CdO} distances, the E_{3bd} value fell off with increasing distance between the two H_2O molecules. The E_{3bd} function can be expressed by equation 4,

$$E_{3bd} = \begin{cases} F \exp - G(r_{CdO_i} + r_{CdO_j}) \times \exp(-Hr_{ij}) \left[(R_{CL} - r_{CdO_i})^2 (R_{CL} - r_{CdO_j})^2 \right]; R_{CaO_i} < R_{CL} \;\&\; R_{CaO_j} < R_{CL} \\ 0; R_{CaO_i} > R_{CL} \; or \; R_{CaO_j} > R_{CL} \end{cases} \quad (4)$$

where F, G, and H are fitting parameters, r_{ij} is the distance between two oxygens of H_2O molecules, and R_{CL} is the cutoff limit of 6.0 Å for the 3-body correction function. A total of 6563 configurations were generated for SCF-energy calculations of $[Cd(H_2O)_2]^{2+}$. The analytical function of equation 4 was fitted to the E_{3bd} values by a least-squares optimization, and the final parameters are given in Table 1. The average absolute residual of the fit was 0.19 kcal mol^{-1}.

Table 1. Parameters for two-body potential and three-body correction function of Cd(II)-water interactions.

2-body					
	Atom	A (kcal/mol)$^{-5}$	B (kcal/mol)$^{-8}$	C (kcal/mol)$^{-9}$	D (kcal/mol)$^{-12}$
Cd	O	-5037.21	108456.03	-144047.88	46229.16
	H	-1650.12	53426.47	-86093.13	51897.80
3-body					
		F (kcal/mol Å^{-4})	G(Å^{-1})	H(Å^{-1})	
H_2O–Cd(II)–H_2O		0.4825593	0.1344984	0.5990947	

Standard MD simulation

The MD simulation method applied in this study was described in detail in a previous paper [16] and will only be briefly reviewed here. The modeled systems consisted one Cd(II) ion plus 499

solvent molecules in a cubic box of 15065.6 Å^3 subjected to periodic boundary conditions. The simulations were performed in the *NVT* ensemble with a time step of 0.2 fs. The density of the simulation box was set to the experimental value of pure water at 298.16 K (0.997 g cm^{-3}). Long range interactions were treated by the reaction field method [34]. The CF2 model was used for the intermolecular potential between H_2O molecules, and the intramolecular potential of H_2O developed by Bopp *et al*. was employed to reproduce correctly liquid-phase vibrational frequencies [35]. In order to construct the initial configuration, the O atoms of H_2O were placed in the simulation box according to the face-centered cubic lattice. The H atoms were arranged with random configuration of H_2O molecules. A total of 400,000 steps (80 ps) were first processed using only the 2-body potential, and the system was confirmed to be energetically equilibrated. A further 400,000 steps (80 ps) were sampled to evaluate structural properties. The simulation was continued for further 400,000 steps (80 ps) of equilibration after the inclusion of the 3-body correction. All energies were confirmed to become stable within 5 ps of equilibration. A further 1,000,000 steps (0.2 ns) simulation was carried out for statistical sampling.

Umbrella-sampling MD simulation

The umbrella-sampling simulation applied in this study is described in detail in [19]. The system is composed of one divalent metal ion and 499 water molecules.

A randomly chosen water from the second hydration shell was made to enter the first hydration under the influence of the umbrella potential V_{umb} (Figure 1):

$$V_{\text{umb}}(r_o) = \frac{k}{2}(r_{ob} - r_o)^2 \tag{5}$$

where r_o is the instantaneous Cd–O distance between Cd(II) and a water molecule in the second hydration shell. The parameter k denotes the force constant and r_{ob} is the restrained Cd–O distance. The distance r_o was varied between 4.5 Å and 2.0 Å to cover the full range between second and first hydration shells. The force constant k was adjusted according to r_o, i.e. k was set to high values close to the transition state and to small values at minima in the PMF. The unbiased probability distribution $\langle\rho(r_o)\rangle$ was obtained by the WHAM [25-27] method to calculate the PMF according to equation 6

$$W(r_o) = -k_{\text{B}}T \ln\langle\rho(r_o)\rangle + C \tag{6}$$

where k_{B} is the *Boltzmann constant*, T the absolute temperature, and C an arbitrary constant. An estimate for the reaction rate constant k_{ex} may then be determined from the free energy difference $\Delta G^{\ddagger}$ between ground and transition state via the classical *Eyring equation* (equation 7)

$$k_{\text{ex}} = \kappa \frac{k_B T}{h} \exp\left(-\frac{\Delta G^{\ddagger}}{\text{RT}}\right) \tag{7}$$

where κ is the transmission coefficient, k_{B} is the *Boltzmann constant*, h is the *Planck constant*, R is the gas constant, and T is the *absolute temperature*.

The simulation protocol was the same as in the standard MD simulation. The starting configuration of the system was taken from the last configuration of the standard simulation obtained using the corrected 2-body potential. In total, 15 independent MD simulations were carried out with 200 ps each reserved for data collection after the system was allowed to reach equilibrium within 2 ps.

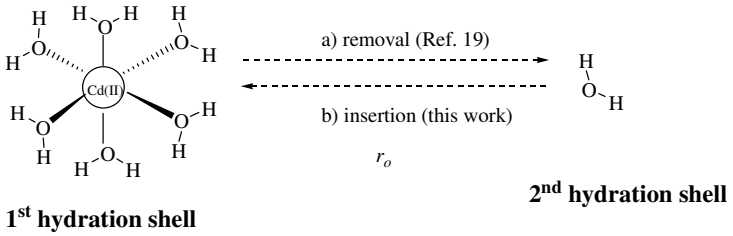

Figure 1. a) Removal of a water molecule from and b) addition to the first hydration shell.

RESULTS AND DISCUSSION

Structural properties

Simulations with only Cd(II)–H_2O pair potential

Results obtained from simulations with only pair-potential are show in Figures 2-4. The simulations with only pair potential resulted a coordination number of 8. The O–Cd(II)–O angular distributions show unrealistic orientation as a result of the large number of water molecules located in the first hydration shell. It is obvious, therefore, that the pair potential is inadequate and at least 3-body corrections are mandatory to correctly describe the hydration structure of Cd(II) ion.

Simulations including three-body corrections for Cd(II)–($H_2O)_2$

The Cd(II)–O and Cd(II)–H radial distribution functions (RDF), and their running integration numbers obtained from the standard MD simulation are displayed in Figure 2. The first Cd(II)–O RDF peak which is related to the first hydration shell reaches its maximum at 2.36 Å and the second peak related to the second hydration shell reaches its maximum at 4.78 Å, clearly separated from the first hydration sphere. Between the first and second shells, it goes to zero implying slow inter-shell water exchange processes. However, the fact that the Cd(II)–O RDF does not go down to zero once the second hydration shell is formed, suggests that this shell must easily interchange water molecules with outer hydration spheres or the bulk.

Cd(II)–H RDF has two peaks, the first one centered at 3.09 Å. The shift of the Cd(II)–H RDF to larger distances with respect to the corresponding Cd(II)–O RDF shows that especially in the first shell, the water molecules are well oriented to obey the dominant ion-water interactions with the oxygen atoms pointing to the ion. Some characteristic values for Cd(II)–O and Cd(II)–H radial distribution functions are listed and compared with results obtained from experimental and theoretical investigations in Table 2.

The coordination number distribution (CND) probability obtained by the standard MD simulation is shown in Figure 3. In the first coordination sphere, the coordination number 6 is observed in agreement with experimental and other simulations results (Table 2).

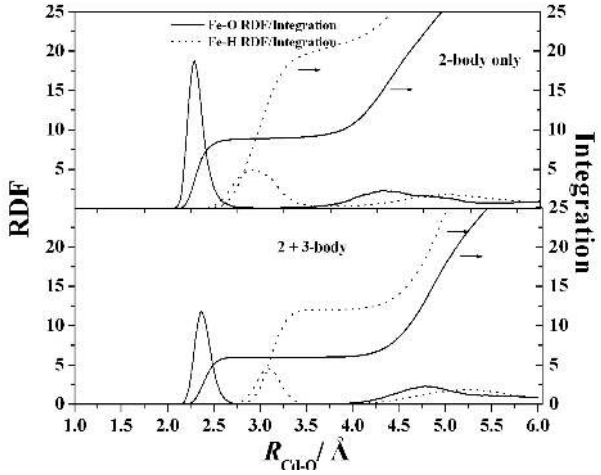

Figure 2. Cd(II)–O and Cd(II)–H radial distribution functions and their running integration numbers.

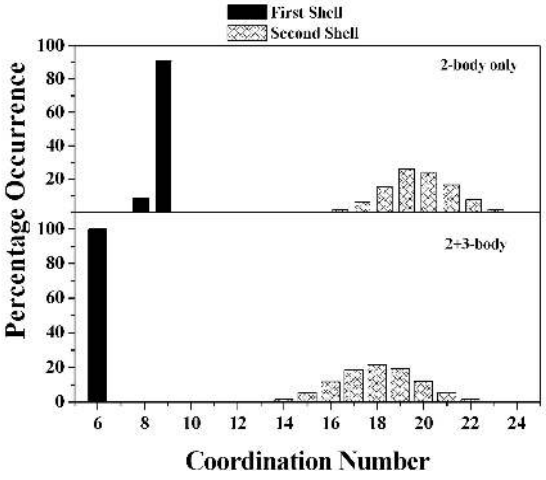

Figure 3. First and second-shell coordination number distribution of hydrated Cd(II).

The probability of finding O–Cd–O angle (θ) in the first hydration shell, the first shell angular distribution function (ADF), obtained from the standard simulation is shown in Figure 4 as a function of 1– *cos* θ. Two well-defined peaks can be observed at the peak maxima of 90º and 180º. This result point out that the hydration geometry around the Cd(II) ion is on average a 6-coordinate octahedral supporting the above observation and in agreement with many experimental results (Table 2).

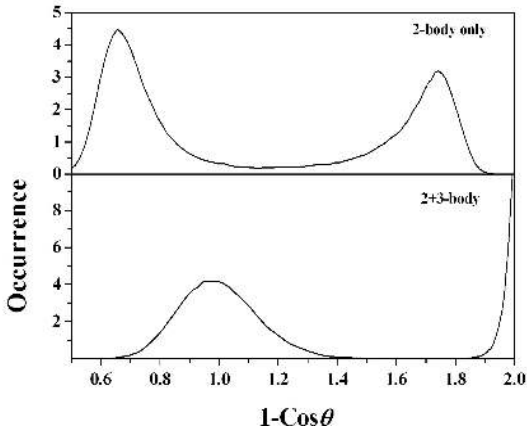

Figure 4. First-shell angular distribution functions for O–Cd–O (θ) in the first hydration shell of the Cd(II) ion as a function of $1-cos\theta$.

Table 2. Hydration structure parameters of the Cd(II) ion in water determined by standard molecular simulation and experimental methods.

Solute	Ion water ratio or molarity	r_{M_1}	r_{n_1}	n_1	r_{M_2}	r_{n_2}	n_2	Method	Ref.
Cd^{2+}	1 M	2.29		6				XD	[36]
$CdCl_2$	1.26 M	2.37		4				XD	[37]
$CdSO_4$	2 M	2.32		5.2	4.36		11.9	XD	[38]
$Cd(ClO_4)_2$	2.1 M	2.31		6				XD	[6]
$Cd(ClO_4)_2$	2.4 M	2.29		6				XD	[6]
$Cd(H_2PO_4)_2$	1 M	2.30		5.1	4.33			XD	[39]
$Cd(NO_3)_2$	4.54 M	2.27		5.7				XD	[40]
Cd^{2+}	1/499	2.35	3.02	6.0	4.93	5.29	12.2	3-body MD	[41]
Cd^{2+}	1/499	2.33	2.78	6.0	4.84	5.27	11.7	QM/MM–MD	[41]
$Cd(H_2O)_{18}^{2+}$		2.34			4.51			RHF/HF/6-31+G*	[42]
$Cd(H_2O)_6^{2+}$	1/6	2.34	-	6.0	-	-	-	RHF/DZP	This work
Cd^{2+}	1/499	2.36	3.09	6.0				3-body MD	This work

r_{M_1}, r_{M_2} and r_{n_1}, r_{n_2} are the distances of the first and second maximum and the first and second minimum in Å. n_1 and n_2 are the average coordination numbers of the first and second hydration shell, respectively.

The average structure of the water molecules in the first shell is investigated *videlicet* the bond distance and angle distributions and are depicted in Figure 5a and b, respectively. The highest probabilities for the bond length and angle distributions are 0.978 Å and 97.58°, respectively. The bond length is shifted to larger value and the bond angle to smaller value as compared to the reference values of the CF2 water model. Obviously, first shell waters are polarized by the presence of the Cd(II) ion.

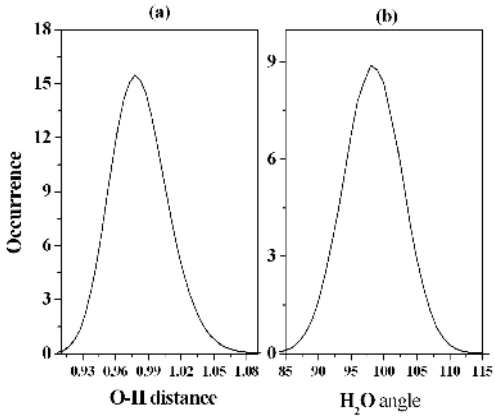

Figure 5. a) Bond length and b) angle distributions of the water molecules in the first shell.

Potential of mean force (PMF) and water exchange rate constant

Water exchange between the hydration shell of ions and the bulk is fundamental for the reactivity of the ions. In Figure 6, the PMF profile for Cd(II) ion as function of Cd(II)–O distance of a water molecule from the second hydration shell is depicted. The PMF has characteristic shape with a first minima at 2.36 Å that corresponds to the average Cd(II)–O distance for the first hydration shell, in agreement with the value obtained by the standard MD simulation (Table 2). The second minimum describes a recovered 6-coordinate octahedral hydration first shell, however, at this point a water molecule had left the first shell and replaced by the biased water molecule from the second shell.

The PMF maxima corresponding to the transition state of the water-exchange process is located at 3.17 Å. The free energy of activation ($\Delta G^{\ddagger}$), the energy difference between the ground state (first PMF minimum) and the transition state (first PMF maximum), is 23.4 kcal mol^{-1}. According to the transition-state theory (equation 7), the water exchange rate constant k_{ex} for Cd(II) ion at 298.16 K is 4.9 x 10^{8} s^{-1}, assuming a transmission coefficient, κ, to be unity. The experimental k_{ex} value is reported to be almost 3 x 10^{8} s^{-1} on the basis of the complexation rate measured by the ultrasonic absorption technique [43]. The result obtained in this study, therefore, considering the uncertainty of k and the simplicity of the potential functions used in this study, is quite reasonable.

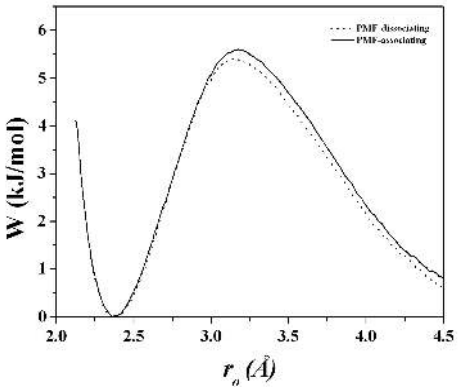

Figure 6. Potential of mean force (PMF) for water exchange process around Cd(II) ion.

The absence of intermediate in the PMF (Figure 6) suggests that the water exchange process is taking place via interchange (I) mode of mechanism in agreement with the result obtained in a previous study [19].

CONCLUSIONS

Ab initio two-body potentials are definitely inadequate to describe the hydration structure of Cd(II) ions. The inclusion of 3-body effects reduces the average first shell coordination numbers from 8 to 6. This result suggests that any successful simulation of doubly charged transition metal such as Cd(II) must include at least three-body effects to give correct structural parameters. The first shell coordination numbers and ion-ligand distances thus obtained with the standard MD simulation including 3-body effects are in good agreement with experimental data. The water exchange rate constant obtained is reasonable given the unknown transmission coefficient and the assumptions made in constructing the Cd(II)-water potential functions. Further, the results obtained from the umbrella-sampling simulation demonstrate that the simply constructed ion-water potential is useful not only for the study of structural parameters but also for the study of water-exchange reactions around metal ions.

AKNOWLEDGEMENTS

Part of this research work was done at Laboratory of Analytical Chemistry, Graduate School of Science, Nagoya University, Japan while the author was postdoctoral fellow of the Japan Society for the Promotion of Science (JSPS) and is grateful to (JSPS) for the fellowship. The author is also grateful to the Department of Chemistry, Addis Ababa University for providing computational facility.

REFERENCES

1. Marcus, Y. *Ion Solvation*, John Wiley and Sons: Chichester, U.K.; **1986**; Chapters 4 and 6.
2. Burger, K. *Solvation, Ionic and Complex Formation Reactions in Non-Aqueous Solvent*s Elsevier: Amsterdam; **1983**; Chapter 6.
3. Burgess, J. *Metal Ions in Solution*, John Wiley and Sons: Chichester, U.K.; **1978**.
4. Creighton, T.E. *Proteins: Structure and Molecular Properties*, 2nd ed., W.H. Freeman and Co.: New York; **1993**.
5. Babu, Y.S.; Sack, J.S.; Greenough, T.J.; Bugg, C.E.; Means, A.R.; Cook, W.J. *Nature* **1985**, 315, 37.
6. Ohtaki, H.; Radnai, T. *Chem. Rev.* **1993**, 93, 1157.
7. Helm, L.; Merbach, A.E. *Chem. Rev.* **2005**, 105, 1923.
8. Rotzinger, F.P. *Chem. Rev.* **2005**, 105, 2003.
9. Marini, G.W.; Liedl, K.R.; Rode, B.M. *J. Phys. Chem. A* **1999**, 103, 11387.
10. Kowall, T.; Foglia, F.; Helm, L.; Merbach, A.E. *J. Am. Chem. Soc.* **1995**, 117, 3790.
11. Marx, D.; Sprik, M.; Parrinello, M. *Chem. Phys. Lett.* **1997**, 273, 360.
12. Kerdcharoen, T.; Liedl, K.R.; Rode, B.M. *Chem. Phys.* **1996**, 211, 313.
13. Martínez, J.M.; Cobos, J.H.; Martin, H.S.; Pappalardo, R.R.; Blake, I.O.; Sánchez Marcos, E. *J. Chem. Phys.* **2000**, 112, 2339.
14. Inada, Y.; Mohammed, A.M.; Rode, B.M.; Loeffler, H. *J. Phys. Chem. A* **2002,** 106, 6783.
15. Iglesias-Yagüe, J.; Mohammed, A.M.; Loeffler, H.H.; Rode, B.M. *J. Mol. Struct.*: *Theochem* **2003**, 620, 15.
16. Mohammed, A.M.; Loeffler, H.H.; Inada, Y.; Funahashi, S. *J. Mol. Liq.* **2005**, 119, 55.

17. Inada, Y.; Mohammed, A.M.; Rode, B.M.; Loeffler, H. *J. Phys. Chem. A* **2002**, 106, 6783.
18. Remsungnen, T.; Rode, B.M. *Chem. Phys. Lett.* **2004**, 385, 491.
19. Inada, Y.; Mohammed, A.M.; Loeffler, H.H.; Funahashi, S. *Helv. Chim. Acta* **2005**, 88, 461.
20. Loeffler, H.H.; Mohammed, A.M.; Inada, Y.; Funahashi, S. *J. Comput. Chem***. 2006**, 27, 1944.
21. Loeffler, H.H.; Inada, Y.; Funahashi, S. *J. Phys. Chem. B***. 2006**, 110, 5690.
22. Armunanto, R.; Schwenk, C.F.; Bambang Setiaji, A.H.; Rode, B.M. *Chem. Phys*. **2003**, 295, 63.
23. Valleau, J.P.; Torrie. G.M. *Chem. Phys. Lett.* **1974**, 28, 578.
24. Valleau, J.P.; Torrie. G.M. *Statistical Mechanics*, *Part A: A Guide for Monte Carlo for Statistical Mechanics*, Berne, B.J. (Ed.); Plennum Press: New York; **1977**.
25. Kumar, S.; Rosenberg, J.M.; Bouzida, J.D.; Swendsen, R.H.; Kollman, P.A. *J. Comput. Chem.* **1995**, 16, 1339.
26. Kumar, S.; Bouzida, J.D.; Swendsen, R.H.; Kollman, P.A.; Rosenberg, J.M. *J. Comput. Chem.* **1992**, 13, 1011.
27. Roux, B. *Comput. Phys. Commun.* **1995**, 91, 251.
28. Frisch, M.J.; Trucks, G.W.; Schlegel, H.B.; Scuseria, G.E.; Robb, M.A.; Cheeseman, J.R.; Zakrzewski, V.G.; Montgomery, J.A. Jr.; Stratmann, R.E.; Burant, J.C.; Dapprich, S.; Millam, J.M.; Daniels, A.D.; Kudin, K.N.; Strain, M.C.; Farkas, O.; Tomasi, J.; Barone, V.; Cossi, M.; Cammi, R.; Mennucci, B.; Pomelli, C.; Adamo, C.; Clifford, S.; Ochterski, J.; Petersson, G.A.; Ayala, P.Y.; Cui, Q.; Morokuma, K.; Salvador, P.; Dannenberg, J.J.; Malick, D.K.; Rabuck, A.D.; Raghavachari, K.; Foresman, J.B.; Cioslowski, J.; Ortiz., J.V.; Baboul, A.G.; Stefanov, B.B.; Liu., G.; Liashenko, A.; Piskorz, P.; Komaromi, I.; Gomperts, R.; Martin, R.L.; Fox, D.J.; Keith, T.; Al-Laham, M.A.; Peng, C.Y.; Nanayakkara, A.; Challacombe, M.; Gill, P.M.W.; Johnson, B.; Chen, W.; Wong, M.W.; Andres, J.L.; Gonzalez, C.; Head-Gordon, M.; Replogle, E.S.; Pople, J.A. *Gaussian 98 Revision A.11*., Gaussian., Pittsburgh PA, **2001**.
29. Hurley, M.M.; Pacios, L.F.; Christiansen, P.A.; Ross, R.B.; Ermler, W.C. *J. Chem. Phys*. **1986**, 84, 6840.
30. Dunning, T.H. Jr. *J. Chem. Phys.* **1970**, 53, 2823.
31. Kuchitsu, K.; Morino, Y. *Bull. Chem. Soc. Jpn.* **1965**, 38, 814.
32. Lemberg, H.L.; Stillinger, F.H. *J. Chem. Phys.* **1975**, 62, 1677.
33. Stillinger, F.H.; Rahman, A. *J. Chem. Phys.* **1978**, 68, 666.
34. Allen, M.P.; Tildesley, D.J. *Computer Simulations of Liquids*, Clarendon, Press: Oxford, U.K.; **1987**.
35. Bopp, P.; Jancsó, G.; Heinzinger, K. *Chem. Phys. Lett.* **1983**, 98, 129.
36. Bol, W. Gerrits, G.J.A.; van Panthaleon van Eck, C.L. *Appl. Crystallogr.* **1970**, 3, 486.
37. Caminiti, R.; Licheri, G.; Piccaluga, G.; Pinna, G.; *Z. Naturforsch.* **1980**, A35, 1361.
38. Caminiti, R. *Z. Naturforsch.* **1981**, A36, 1062.
39. Caminiti, R. *J. Chem. Phys.* **1982**, 77, 5682.
40. Caminiti, R.; Cucca, P.; Radani, T. *J. Phys. Chem.* **1984**, 88, 2382.
41. Kritayakornupong, C.; Plankensteiner, K.; Rode, B.M. *J. Phys. Chem. A* **2003**, 107, 10330.
42. Rudolph, W.W.; Pye, C.C. *J. Phys. Chem. B* **1998**, 102, 3564.
43. Eigen, M. *Pure Appl. Chem.* **1963**, 6. 97.